

# Dynamic Analysis and Optimization of Soft Robotic Fish Using Fluid-Structural Coupling Method

Wenjing Zhao, Aiguo Ming, Makoto Shimojo, *Member, IEEE*

**Abstract**— Aiming to design a soft robotic fish with more natural, more flexible and high-performance movements through biomimetic method, we are developing a soft robotic fish with body/caudal fin (BCF) propulsion by using piezoelectric fiber composite (PFC) as actuator. Compared with conventional rigid robotic fish, the design and control of the soft robotic fish are difficult and hard to reveal its dynamic performances due to the large deformation of flexible structure and complicated coupling dynamics with fluid. That's why the design and control method of the soft robotic fish has not been established, and we need to study it by considering the interaction between flexible structure and fluid. In this paper, fluid-structural coupling analysis based on acoustics method is applied to consider the fluid effect and predict the dynamic responses of soft robotic fish using PFC in fluid. Basic driving and governing equations of soft robotic fish in the fluid are firstly described. Then the numerical acoustics coupling analysis is performed. The calculated results are congruent well with experiments on dynamic responses. Finally, based on this coupling method, a new prototype of soft robotic fish is proposed by optimization for improvement.

## I. INTRODUCTION

Biomimetic robots make a lot of irreplaceable contributions in human life with the development of interdisciplinary sciences, including the science of electronic information and biological technology [1]-[4]. Many researchers concentrate on the field of biomimetic robots, especially on the development of biomimetic robotic fish by mimicking the real creatures [4]-[10] such as Robotuna of MIT, Essex robotic fish in London aquarium, robotic fish with rigid tail of MSU, snake-like robot (AmphiBot) of EPFL, SSSA Lamprey robot, FILOSE robot from Tallinn University, NanyangAwana (NAF-I), robotic eel of Methran Mojarrad group, and so on. In these researches, the fishes become one of the focuses to be mimicked due to their high efficiency, good flexibility and maneuverability. Some fishlike robots are available for the seabed rescue, exploration, observation and other special underwater work, currently [1]-[5].

In these fishlike robots, the propulsion methodologies are various, such as by conventional motor mechanism [6]-[9] and by artificial muscle mechanism [10]-[15]. Among the propulsion mechanisms, the motor mechanism is simple but lack of flexibility with high energy cost. The robots usually have large size and heavy weight with rigid materials and complex control system [16]. Artificial muscle mechanism

using electrostatic film, shape memory alloy (SMA), PZT film, ionic polymer petal composite (IPMC), giant magnetostrictive alloy (GMA) or PFC is soft and flexible. The robotic fish with artificial muscle mechanism can obtain relatively good propulsion like real fish.

When designing a soft robotic fish, a surrounding fluid must be considered. The fluid increases the system mass, stiffness and damping, changes the mechanical dynamic characteristics of the contained structure. To fully study the dynamic response of the soft robotic fish, we must take into account the dynamic interaction between the fluid and robot structure, and model the coupling mechanism accurately for fluid-structure interaction (FSI) analysis [17].

A broad class of FSI problems involves a fluid without significant flow and the main concern in the fluid is the pressure wave propagation. The acoustics fluid-structure coupled method considering the acoustic pressure can be used to solve these FSI problems and predict vibrational modes and transient responses of the structures in the fluid. M. B. Xu [18], S. M. Ai, et al. [19] studied the vibration response of underwater cylindrical shells through the fluid-structure coupled acoustic analysis. D. J. Nefske, et al. analyzed the vehicle vibration by a coupled finite element model [20]. Carl Howard presented a vibration analysis of an infinite duct divided by a thin panel through a coupled structural acoustic analysis [21]. H. Djojodihardjo applied the acoustic-structure interaction technology with finite element method (FEM) into spacecraft structures [22]. These studies provide a basis of flow formulation and boundary conditions of fluid-structural coupling analysis. However, the coupling problem is very difficult to be solved and design method of the soft robotic fish has not been established due to the large deformation of flexible structure and complicated coupling dynamics. It motivates us to investigate the design and control of the soft robotic fish by analytical simulation on coupling effect between the soft structure and fluid.

Due to the relatively higher efficiency, higher acceleration and faster swimming speed, the BCF propulsion is more favorite in the design. In the present research, we utilize the PFC as soft actuator to develop a soft robotic fish with BCF propulsion. PFC can be constructed to a simple structure with high efficiency of energy conversion and large response of displacement. In this paper, the acoustics fluid-structural coupling analysis using FEM is applied to predict the dynamic vibration response of the soft robotic fish in the fluid. Well-established experiments are performed to validate its vibration response with coupling method. Finally, a new optimal structure and prototype are proposed by this established coupling method for improvement.

Wenjing Zhao is with the Department of Mechanical Engineering and Intelligent Systems, The University of Electro-Communications, Tokyo 182-8585, Japan (e-mail: zhaowenjing@rm.mce.uec.ac.jp)

Aiguo Ming and Makoto Shimojo are with the Department of Mechanical Engineering and Intelligent Systems, The University of Electro-Communications, Tokyo 182-8585, Japan (e-mail: ming@mce.uec.ac.jp; shimojo@mce.uec.ac.jp).

The aim of this study is not only to develop a soft robotic fish by PFC, but to establish the coupling method of underwater robot for propulsion improvement. By the verified coupling method, the dynamic vibrational frequencies and mode shapes of a structure in the fluid can be predicted and utilized to design different propulsion. Various propulsion such as caudal fin, snake-like body or pectoral fin propulsion can be generated based on different vibrational modes in the fluid. The corresponding oscillating, undulating or flapping motion also can be expected by different mode actuation.

## II. MATERIALS AND BASIC THEORY

### A. Piezoelectric Fiber Composite

We choose one of typical PFC, macro fiber composite (MFC) [15], as a soft actuator due to its large displacement response and high efficiency. Figure 1 shows the structure and driving model of the MFC. The piezoceramic fiber is embedded in epoxy to make a rectangular plate. The plate is sandwiched by two pieces of polyimide film on which the interdigitated electrodes are placed. Based on thermodynamic theory, when a voltage from -500V to +1500V is applied on MFC, the strain and stress will be generated, and a driving load can be finally obtained by (1). The structure can be expanded and contracted in the direction of the fibers by the driving load [23].

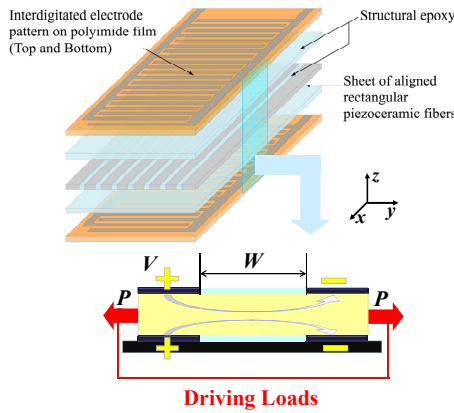


Figure 1. Schematic diagram of structure for MFC

$$\begin{Bmatrix} P_x \\ P_y \end{Bmatrix} = \frac{1}{1 - \nu_{xy}\nu_{yx}} \begin{bmatrix} E_x & E_x \nu_{yx} \\ E_y \nu_{xy} & E_y \end{bmatrix} \begin{Bmatrix} d_{33} \\ d_{31} \end{Bmatrix} \frac{V}{W} \quad (1)$$

where  $E_x$  and  $E_y$  are tensile modulus in the  $X$  and  $Y$  direction, respectively;  $\nu_{xy}$  and  $\nu_{yx}$  are Poisson's ratio;  $d_{33}$  and  $d_{31}$  are piezoelectric constants;  $V$  is voltage applied to MFC;  $W$  is distance between the electrodes of MFC;  $P$  is driving load.

When the MFC combines with a thin elastic plate, it will generate bending or torsion deformation due to resonance. We utilize the resonant bending deformation to design the soft fish robot with BCF propulsion. The carbon-fiber-reinforced polymer (CFRP) is adopted as the thin elastic plate.

### B. Theory of Acoustics Fluid-Structural Coupling

Addressing the acoustic structural interaction problems, the FEM is widely used to predict the dynamic responses of the structure submerged in fluid. The entire problem domain is

divided into elements rather than only bounding surface of the domain. In this paper, we use the FEM to deal with the fluid-structural coupling problem through ANSYS software. Acoustic elements satisfy the required fluid-structural coupling at the interface because they have four DOFs: three for displacement and one for pressure. A consistent matrix coupling is set up between the structural and fluid elements in which strongly coupling causes no convergence problems.

The FSI analysis by ANSYS acoustic program assumes the fluid is ideal fluid and meets the following conditions: firstly, the fluid is non-flowing, inviscid and compressible, but allows only relatively small pressure changes with respect to the mean pressure; secondly, the amplitude in acoustic domain is relatively small for small variation in fluid density; thirdly, there is no heat transfer. The transfer between the wave propagation and thermodynamics is adiabatic.

The interaction between the fluid and structure at the interface causes the acoustic pressure to exert a force applied to the structure and the structural motion produces an effective fluid load. The governing finite element matrix equation in the coupled analysis is shown as (2) [24]. In the coupled system, the fluid damping effect is considered as the external loads of structure rather than damping matrix  $C_s$ . Thus, the external loads of structure  $F_s$  is composed of the driving loads from (1) and the fluid damping effect in the fish robot system. Both structural and fluid loads are transferred at the fluid-structure interface. The nodes on the fluid-structure interface have both displacement and pressure DOF. If  $F_s$  equals zero, (2) will become the equation of coupled modal analysis for the robot.

$$\begin{bmatrix} M_s & 0 \\ \rho R^T & M_f \end{bmatrix} \begin{Bmatrix} \ddot{U} \\ \ddot{P} \end{Bmatrix} + \begin{bmatrix} C_s & 0 \\ 0 & 0 \end{bmatrix} \begin{Bmatrix} \dot{U} \\ \dot{P} \end{Bmatrix} + \begin{bmatrix} K_s & -R \\ 0 & K_f \end{bmatrix} \begin{Bmatrix} U \\ P \end{Bmatrix} = \begin{Bmatrix} F_s \\ F_f \end{Bmatrix} \quad (2)$$

where  $M$ ,  $C$  and  $K$  are structural element mass, damping and stiffness matrix, respectively;  $F$  is external load;  $U$  is displacement;  $P$  is fluid acoustic pressure;  $\rho$  is fluid density; subscripts  $S$  and  $F$  are expressed as solid and fluid domain, respectively.  $R$  is coupling matrix represents the effective surface area associated with each node on the fluid-structure interface. It transfers the fluid pressure on interface to the driving loads on structure in the coupled analysis.

## III. DYNAMIC ANALYSIS AND EXPERIMENTS

### A. Model of the Soft Robotic Fish

The prototype and geometric model of the soft fish robot with BCF propulsion are shown in Fig. 2.

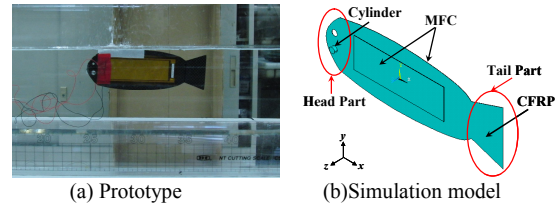


Figure 2. Soft robotic fish

The robot body is made by a CFRP plate and two MFC plates. Two MFC plates sandwich the CFRP plate as the actuator structure for bending deformation propulsion. Steel

cylinder is placed on the head to constrain its motion and increase the displacement of the tail end. This constrained structure is similar to a cantilever beam. The body height is varied toward the tail end and it is smallest at the place where the caudal fin connects to fish body. Low density blowing agent as the float is placed on the top to balance the robot weight in the experiment. The MFC of M-8528-P1 type is adopted [25]. The total length of the robot is 167mm. Table I shows the robot's material properties.

TABLE I. MATERIAL PROPERTIES OF THR SOFT ROBOTIC FISH

Item	Material	
	Steel	CFRP
Density ( $\text{kg/m}^3$ )	7850	1643
Elastic Modulus (GPa)	20	20.5
Poisson's ratio	0.3	0.3
Thickness (mm)	2.5	0.2

### B. Structural Dynamic Analysis

Structural dynamic vibration analysis and transient analysis (time-history analysis) are used to determine the dynamic responses of the soft robot. Three-dimensional (3-D) acoustic fluid element FLUID30 is used to model the fluid domain and the interface in the FSI analysis. It has eight corner nodes and each node has four DOFs. 3-D solid element SOLID186 is adopted to describe the robot structure domain. As shown in Fig. 3, a spherical surface is set as the boundary of the fluid domain, whose diameter is 220mm. A pressure load is applied on the outer border of the fluid domain. The soft robot is placed in the middle of the static fluid and its finite element model is presented in Fig. 3(b). The number of the total grid nodes for whole computational domain is 140,886 and number of the total elements is 244,105.

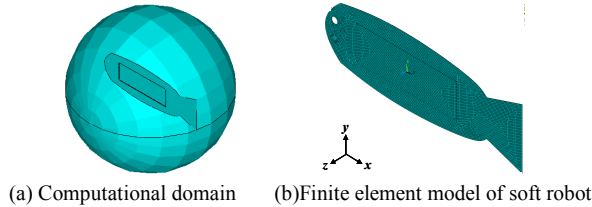


Figure 3. Model of the soft robot fish in the fluid

Due to the high voltage of MFC, the Fluorinert Electronic Liquid FC3283 is adopted to describe the properties of the fluid, whose density is  $1820 \text{ kg/m}^3$ . It is a fully-fluorinated liquid. Its composition will not shift or fractionate with time. It keeps fluid loss to a minimum and insures the fluid transport properties are stable. Based on above computational domain, the coupling vibration analysis of the soft robot is firstly studied. There isn't any fixed support on robot. The vibrational frequencies of the soft robot in the fluid are shown in Table II, where the first six mode frequencies are presented.

TABLE II. VIBRATIONAL FREQUENCIES OF SOFT ROBOT IN THE FLUID

Item	Frequency (Hz)					
Mode	1	2	3	4	5	6
Robot	5.99	16.55	24.99	36.3	43.8	57.8

When the geometry size of the fluid is changed, there is almost no influence on vibrational frequencies. The change in fluid volume has little effect on natural frequencies of the

robot. The far-field condition is applied to the fluid successfully. The corresponding vibrational modes are shown in Fig. 4, where we mainly concern the bending deformation and the first two bending modes are described. The experimental results are measured by the high speed camera. The first torsion mode occurs on the caudal fin at 16.55Hz. When the driving frequencies are about 6Hz and 25Hz, we obtain the first and second bending mode, respectively. They have the similar mode shapes at the corresponding frequencies between the simulation and experiment. The first bending mode is similar to oscillating deformation and the largest displacement is gotten at the tail end. For the second bending mode, the deformation is similar to S-shape. The minimum deformation all happens at the position where the distance from the edge of the head is about one-third of body length. The calculated results on vibrational frequencies and bending modes are congruent to the experiments.

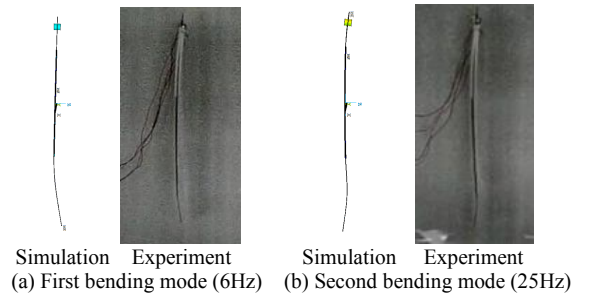


Figure 4. Vibrational modes on bending deformation of the soft robotic fish

Then the transient analysis is carried out to determine the displacement response of the soft robot with a time-varying driving load in the fluid. There isn't any fixed support on robot. The driving load from (1) in sine wave is applied to robot. The main propulsion mode of the soft robot is first bending mode and we mainly focus on it. The maximum deformation occurs at the caudal fin end. Thus, the displacement of the tail end is used to describe the deformation response of the soft robot. We adopt the results of 3Hz, where the robot has the good flexible fishlike movement due to suitable swimming number  $S_w$  [26] and Strouhal number  $S_r$ , to make the description. The displacement of the tail end in one cycle is presented in Fig. 5.

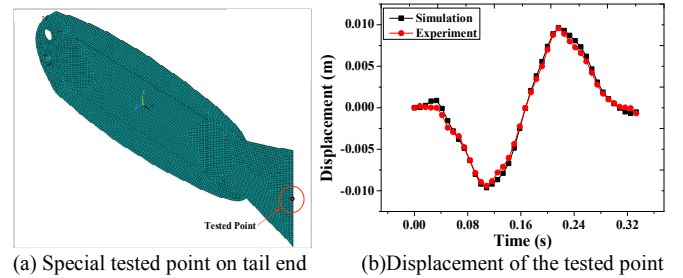


Figure 5. Displacement of the tail end of the soft robot

The special tested point shown in Fig. 5(a) is used to describe the displacement response in the current research. There is very similar displacement curve occurs in the simulation and experiment. The caudal fin makes the oscillating motion similar to a sine wave. The maximum displacement of the tail end is about 20mm. Compared with the experiment about 19mm, there is very small difference. As

a conclusion, the simulation coincides with experiment well. The method of FSI analysis is verified reasonable by the experiment, and efficient bending propulsion is realized successfully on prototype. The displacement response of the soft robot in the fluid is determined well through this method. The coupling method can be used to evaluate the vibration characteristics or propulsion modes of the soft robot in the fluid. It provides a way for further robot optimization on dynamic propulsion in the design of underwater soft robots.

#### IV. STRUCTURE OPTIMIZATION

Structure optimizations are carried out to improve the dynamic characteristics of the soft robot by coupling method. The propulsion with first bending mode is concerned.

Keulegan-Carpenter number  $KC$  [27], also called the period number, is related with swimming speed  $V$ , tail beat frequency  $f$  and maximum lateral displacement of the caudal fin  $A$ . It can be expressed by  $KC=V/(fA)$ , is equal to the reciprocal of the Strouhal number  $S_r$  in form. It is used for describing the relative importance of the drag force over inertial force for objects oscillating in a stationary fluid. For small  $KC$ , the inertia dominates, while the drag force is important for large  $KC$ . In order to develop a soft robotic fish with inertia type, we need to decrease the  $KC$ . Thus, the oscillating amplitude of the caudal fin, that is, the bending displacement of the tail end, should be increased when the frequency is decided. The tested point in Fig. 5(a) is also adopted for describing the displacement of the tail end. The driving load of 3Hz in sine wave is applied for comparison.

The caudal fin shape, head weight volume and body thickness of the soft fish robot play an important role in the movement [28], and they are optimized for improvement. The dashed lines in Fig. 6 describe the locations of the optimization on robot structure. The caudal fin shape is firstly presented, where the height of caudal peduncle and caudal fin are considered. At first, the height of caudal peduncle where the caudal fin connects to the fish body is optimized. The displacement of the tail end in one cycle is shown in Fig. 7(a). The caudal peduncle height is ranged from 3mm to 30mm. For different height, there are almost identical tracks similar to sine wave occur. The caudal peduncle height is in inverse proportion to the displacement of the caudal fin end. The maximum displacement about 48.3mm occurs when the caudal peduncle height is 3mm. It is greatly larger than the old robot with 20mm. The caudal peduncle height of 3mm is used for further optimization.

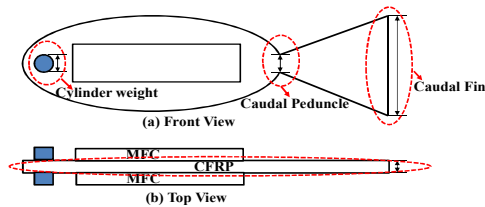
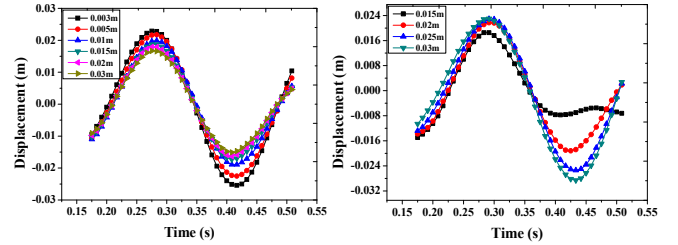


Figure 6. Locations of the optimization for soft robotic fish

Then the caudal fin height is optimized in the range of 15mm~30mm based on caudal peduncle height of 3mm. The displacement results of the tail end in one cycle are shown in Fig. 7(b). Due to the weakened stiffness, the deformation track

has a little irregular when the height is 15mm. If the height is 30mm, the displacement reaches the maximum value about 52mm. The caudal fin height is proportional to the displacement of the tail end. The optimal height is 30mm.



(a) different caudal peduncle heights (b) different caudal fin heights

Figure 7. Displacement of the tail end at different heights of caudal peduncle and caudal fin

CFRP plate is the main component of the robot. Its thickness is important for large deformation. Through the optimal height of the caudal fin shape, the robot is optimized in the thickness range of CFRP from 0.1mm to 1mm. Figure 8 shows the displacement results of the tail end in one cycle. When the thickness is 0.2mm, the maximum deformation occurs. The CFRP with 0.2mm thickness is adopted.

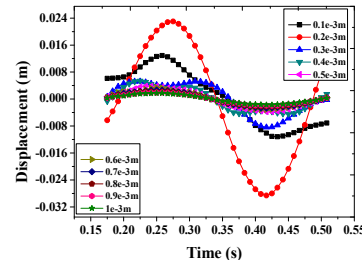


Figure 8. Displacement of the tail end at different thicknesses of CFRP

Cylinder weight is placed on the head to constrain the head motion for larger displacement of the tail end. The optimizations of cylinder volume are carried out in the radius range of 1mm~7mm. Figure 9 presents the displacement of the tail end and head tip at different radii of the cylinder. There are almost identical curves happen at different volumes both on caudal fin end and head tip. The displacement difference among different volumes is small, especially on the head tip. The displacement of the tail end is proportional to the volume of the head cylinder. When the radius is 7mm, it obtains the maximum displacement. The radius of 7mm is optimal.

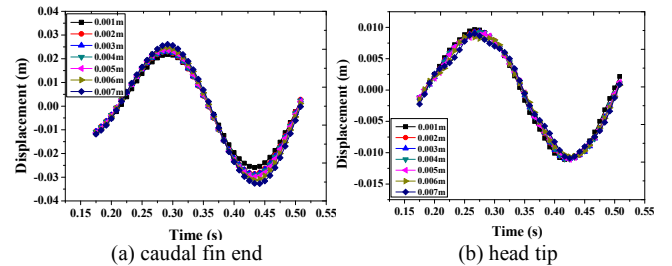


Figure 9. Displacement at different radii of the head cylinder

Finally, caudal peduncle height with 3mm, caudal fin height with 30mm, CFRP with 0.2mm thickness and radius of the head cylinder with 7mm are adopted to design the new soft robot for improvement. Figure 10 displays the new model.



The main body is also made by a CFRP plate and two MFC plates. Cylinder weight is also placed on the head to increase the displacement of the tail end. In the experiment, the blowing agent is also placed on the top to balance the robot weight. The type of the MFC is same to the old robot's.

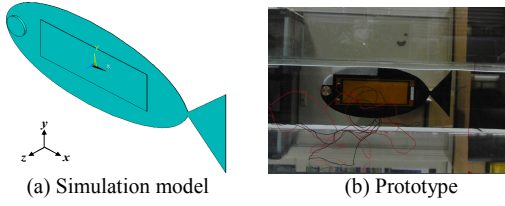


Figure 10. Model of the new soft robotic fish

The bending deformation tracks of the new robot and old robot are shown in Fig. 11. Here we take the results of 3Hz as an example for comparison. The results in quarter of one cycle are presented due to the motion symmetry. The maximum deformation occurs at the tail end for both new and old robot, and the minimum deformation all happens at the position where the distance from the edge of the head is about one-third of body length. They have the similar first bending mode, but the new robot's displacement is larger, meets the desired purpose for large displacement preliminarily. The  $KC$  of the new robot is smaller than the old robot. The inertia will dominate in its movement. The new soft robot has the better fishlike movement performance with larger deformation.

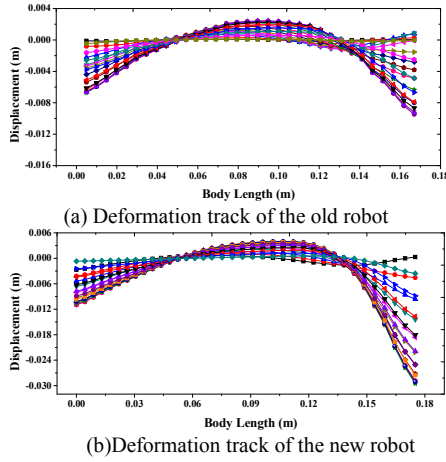


Figure 11. Deformation track of the soft robot in quarter of one cycle

Figure 12 describes the difference of the first bending mode at 3Hz for new soft robot between the simulation and experiment. The results in quarter of one cycle are presented. There is almost same bending mode exists in simulation and experiment. The efficient bending propulsion based on oscillating motion is realized by the coupling method.

Furthermore, the vibrational frequencies of the new soft robot with a free boundary condition are shown in Table III. The first five mode frequencies are presented. Compared with the old robot, the vibrational frequencies of the new soft robot in the fluid are smaller due to the change in structure stiffness and weight. The first bending mode frequency is about 4Hz for new robot and 6Hz for old robot, and its maximum displacement occurs at the tail end. The second bending mode similar to S-shape is obtained at about 20.5Hz for new robot

and 25Hz for old robot. If the frequency is 29Hz, the third bending mode occurs on new robot and we can get the maximum displacement at the head part. When the frequencies are about 11Hz and 37.9Hz, the first and second torsion deformation occur on the new robot, respectively.

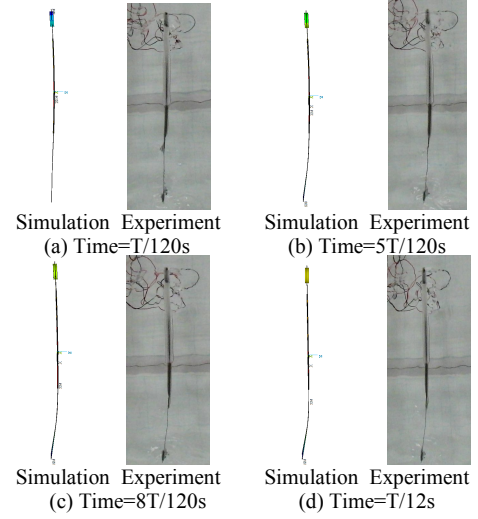


Figure 12. Deformation modes of the new robot in quarter of one cycle

TABLE III. VIBRATIONAL FREQUENCIES OF SOFT ROBOT IN THE FLUID

Item	Frequency (Hz)				
Mode	1	2	3	4	5
Old robot	5.99	16.55	24.99	36.3	43.8
New robot	3.95	10.7	20.5	29.0	37.9

In this research, we mainly concern bending deformation for oscillating or undulating movement. Therefore, the first three bending modes of the new robot are presented in Fig. 13.

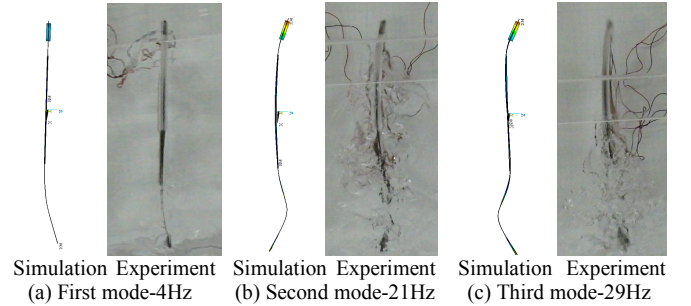


Figure 13. Vibrational modes of the new soft robot

The simulation result of the new soft robot has the similar bending modes with the experiment at the corresponding mode frequencies. When the frequency of first bending mode is applied, the deformation is similar to oscillating propulsion. If the second and third bending modes occur, we can get the undulating propulsion. As a conclusion, the simulation results on bending propulsion modes about frequencies and mode shapes coincide with experimental results well and efficient bending propulsion is realized by the FSI coupling analysis.

The swimming number  $S_w$  and Strouhal number  $S_t$  of the new soft robot at different bending propulsion modes are shown in Fig. 14. The  $S_w$  and  $S_t$  of the new soft robot are larger than the old robot both at the first and second bending propulsion mode. The  $S_w$  of the new robot is much close to 0.6

where the best flexibility and mobility happen compared with the old robot [26]. The  $S_r$  is generally in the range from 0.25 to 0.4 for good fishlike movement performances. For the new soft robot, the  $S_r$  is about 0.4 for both bending propulsion modes. However, the old robot's is less than 0.2 at the first bending mode. The new soft robot has the better propulsion performances similar to those of fishes, and the inertia dominates in the movement due to the smaller  $KC$ .

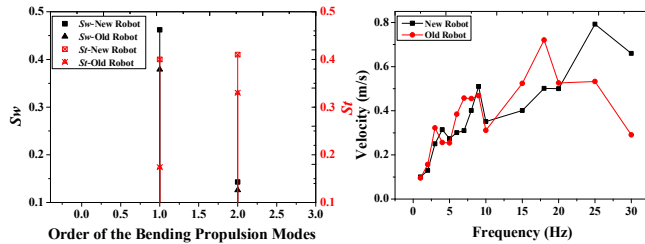


Figure 14.  $S_w$  and  $S_r$  of the new robot at different modes

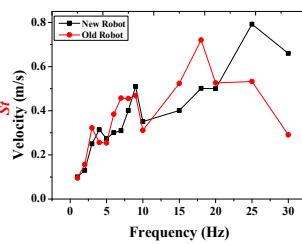


Figure 15. Swimming velocity of the new robot at different frequencies

By focusing on the deformation modes of the new robot in the experiment, the swimming velocity at different frequencies from 1Hz to 30Hz can be obtained in Fig. 15. The similar velocity curve occurs on the new and old robot. However, the maximum swimming velocity of the new robot is larger than the old robot about 0.72m/s. The new soft robot can reach up to about 0.792m/s at 25Hz.

## V. CONCLUSION

In this paper, the dynamic analysis of the soft robotic fish using PFC based on acoustics fluid-structural coupling method is performed to evaluate the dynamic vibration responses of the soft robot in the fluid. The effectiveness and reasonability of this coupling method are validated by comparing with experiment. Finally, a new soft robotic fish is presented by optimization. The efficient body bending propulsion based on oscillation or undulation is realized through the coupling method. The new soft robot has the better propulsion performances similar to those of fishes than the old robot. And the swimming velocity can reach 0.792m/s at 25Hz larger than the old robot. In future, improvement on propulsion performances of the new soft fish robot by coupling method will be done.

## REFERENCES

- [1] E. Kim, Y. Youm, "Design and dynamic analysis of fish robot: Potuna," *Proceedings of the IEEE International Conference on Robotics and Automation*, 2004.
- [2] J. M. Anderson, "The vorticity control unmanned undersea vehicle," *Proceeding of the International Symposium on Seawater Drag Reduction*, 1998, pp. 479–483.
- [3] X. Y. Deng, S. Avadhanula, "Biomimetic micro underwater vehicle with oscillating fin propulsion: system design and force measurement," *Proceedings of the IEEE International Conference on Robotics and Automation*, Barcelona, Spain, 2005, pp. 3312–3317.
- [4] J. M. Kumph, "Maneuvering of a robotic pike," M.S. thesis, Massachusetts Institute of Technology, USA, 2000.
- [5] M. S. Triantafyllou, A. H. Techet, F. S. Hover, "Review of experiment work in biomimetic foils," *IEEE Journal of Oceanic Engineering*, vol. 29, no. 3, pp. 585–593, 2004.
- [6] K. H. Low, C. W. Chong, Chunlin Zhou, "Performance study of a fish robot propelled by a flexible caudal fin," *IEEE International Conference on Robotics and Automation Anchorage Convention District*, Anchorage, Alaska, USA, 2010, pp. 90–95.
- [7] X. Tan, Michael Carpenter, John Thon, Freddie Alequin-Ramos, "Analytical modeling and experimental studies of robotic fish turning," *IEEE International Conference on Robotics and Automation Anchorage Convention District*, Anchorage, Alaska, USA, 2010, pp. 102–108.
- [8] H. S. Hu, "Biologically inspired design of autonomous robotic fish at Essex," *Proceedings of the IEEE SMC UK-RI Chapter Conference on Advances in Cybernetic Systems*, 2006, pp. 1–8.
- [9] Alessandro Crespi, Andr e Badertscher, Andr e Guignard, et al., *AmphiBot I: an amphibious snake-like robot*, *Robotics and Autonomous Systems*, vol. 50, pp. 163–175, 2005.
- [10] Mehran Mojarad, Mohsen Shahinpoor, "Biomimetic robotic propulsion using polymetric artificial muscles," *Proceedings of the IEEE International Conference on Robotics and Automation*, 1997, pp. 2152–2157.
- [11] Z. G. Zhang, N. Yamashita, M. Gondo, et al. "Electrostatically actuated robotic fish: design and control for high-mobility open-loop swimming," *IEEE Transactions on Robotics*, vol. 24, no. 1, pp. 118–129, February 2008.
- [12] S. X. Guo, Y. M. Ge, L. F. Li, S. Liu, "Underwater swimming micro robot using IPMC actuator," *IEEE International Conference on Mechatronics and Automation (ICMA)*, 2006, pp. 249–254.
- [13] Q.L.N. Wilson G V Webb, O. K. Rediniotis, D. C. Lagoudas, "Development of a shape memory alloy actuated biomimetic hydrofoil," *Intelligent Material System and Structure*, vol. 13, no. 1, pp. 35–49, 2002.
- [14] T. Fukuda, H. Hosokai, et al., "Giant magnetostrictive alloy (GMA) application to micro mobile robot as a micro actuator without power supply cable," *Proceeding of Micro Electro Mechanical Systems*, Nara, 1991, pp. 210–215.
- [15] R. Brett Williams and Daniel J. Inman, "An overview of composite with piezoceramic fibers," *Proc. Of the 20th International Modal Analysis Conference*, Los Angeles, CA, 2002.
- [16] K. H. LOW, A. WILLY, "Biomimetic motion planning of an undulating robotic fish fin," *Journal of Vibration and Control*, vol. 12, no. 12, pp. 1337–1395, 2006.
- [17] Bungartz, Hans-Joachim, Sch afer, Michael, eds., *Fluid-structure Interaction: Modelling, Simulation, Optimization*, Springer-Verlag. ISBN 3-540-34595-7, 2006.
- [18] M. B. Xu, "Three method for analysis forces vibration of a fluid-filled cylindrical shell," *Applied Acoustics*, vol. 64, no. 7, pp. 731–752, 2003.
- [19] S. G. Ai, L. P. Sun, "Fluid-structure coupled analysis of underwater cylindrical shells," *Journal of Marine Science and Application*, vol. 7, no. 2, pp. 77–81, 2008.
- [20] S. H. Sung and Donald J. Nefske, "A coupled structural acoustic finite element model for vehicle interior noise analysis," *Transaction of the ASME, Journal of Vibration, Acoustics*, vol. 106, no. 2, pp. 314–318, 1984.
- [21] Carl Howard, "Coupled structural-acoustic analysis using ANSYS," Internal Report of the University of Adelaide, 2000.
- [22] H. Djojodihardjo, "BEM-FEM acoustic-structure interaction for modeling and analysis of spacecraft structures subject to acoustic excitation," *International Conference on Recent Advances in Space Technologies*, 2007, pp. 165–170.
- [23] R. Brett Williams, "Nonlinear mechanical and actuator characterization of piezoelectric fiber composites," Ph.D. dissertation, Virginia Polytechnic Institute and State University, USA, 2004.
- [24] ANSYS Inc., *ANSYS theory reference 12.1*, ANSYS Inc., 2009.
- [25] <http://www.smart-material.com/MFC-product-main.html>.
- [26] I. Tanaka, M. Nagai, *Hydrodynamic of Resistance and Propulsion-Learn from the Fast Swimming Ability of Aquatic Animals*, Ship & Ocean Foundation, 1996, pp. 14–19.
- [27] H. Dutsch, F. Durst, S. Becker, H. Lienhart, "Low-Reynolds-number flow around an oscillating circular cylinder at low Keulegan-Carpenter numbers," *J. Fluid Mech.*, vol. 360, pp. 249–271, 1998.
- [28] H. Kagemoto, et al., "Why do fish have the 'fish-like geometry'?", *Proceedings of... Annual Meeting, Japan Society of Fluid Mechanics*, vol. 29, pp. 395–396, 2010.